

Numerical study of water Infiltration in biochar-amended landfill covers under Extreme Climate

Arwan Apriyono¹, Yuliana¹, Zhongkui Chen² and Viroon Kamchoom^{1,*}

¹Excellent center for green and sustainable infrastructure, Department of Civil Engineering, School of Engineering, King Mongkut's Institute of Technology Ladkrabang (KMUTL), Thailand

²Shenzhen Yanzhi Science and Technology Co., Ltd, Shenzhen 518101, China

*Corresponding author; E-mail address: viroon.ka@kmitl.ac.th

Abstract

The utilization of biochar as an environmentally sustainable material has garnered attention in recent years for its ability to enhance soil properties, such as mechanical and hydraulic characteristics. Nevertheless, a comprehensive understanding of the effects of biochar on water infiltration in landfill covers, especially with regards to variations in rainfall and evaporation patterns, is limited. This study aims to investigate the effects of biochar on soil water infiltration extreme climate. To do this research, finite element analyses were conducted using SEEP/W under a two-dimensional axis-symmetry condition. Both drying and wetting SWRC data from the experiment were fitted with the van Genuchten model and implemented into the numerical models. Moreover, A series of numerical analysis was performed to observe the PWP response during extreme rainfall and evaporation events. The results of this study indicate that the addition of biochar to CDG led to a delay in the response time of water infiltration, reducing the depth of the wetting front and slowing down water infiltration. Furthermore, the addition of biochar can significantly reduce the increasing of PWP during infiltration under extreme climate.

Keywords: Landfill cover, Peanut shell biochar, Granite residual soil, Numerical simulation, Extreme climate

1. Introduction

Water infiltration plays an important role in many aspects of human life such as geotechnical, hydrological engineering and agriculture. It is an undeniable fact that water infiltration may trigger stability and serviceability problems in many earthworks [1]–[3]. Rainfall infiltration alters the behaviour of the soil,

especially its strength due to the increasing pore water pressure, inducing a slope instability problem [4]–[6]. Meanwhile, overwhelming water infiltration during wet season can seriously disturb plant growth and lead to significant yield losses in many crops' species [7]–[9]. Besides, especially in geotechnical engineering, extreme climate will significantly affect several earth structures with respect to crack and infiltration rate alteration [10], [11]. Prolonged drought will trigger notable crack development considering higher soil moisture deficit and soil suction, thus increasing water infiltration rate [12], [13]. Moreover, the increasing of cracks can also rise evaporation considering higher evaporative surface from one-dimensional to three-dimensional pattern [14], [15]. Yet, based on [16], evaporation rate can be double with cracking, compared to initial compacted soil. Controlling water infiltration is thus becoming a challenging topic to address for both researcher and engineer to prevent aforementioned problem, especially under extreme climate.

In the recent past, many studies have investigated the application of biochar to reduce water infiltration. Regarding having an extremely porous structure, biochar can increase soil water retention and decrease soil permeability [17], [18]. As a result, biochar is becoming an alternative material to enhance earthwork stability and provide more sustainable landfill construction that mitigates extreme climate problems. However, to date, the majority of studies examined the impact of biochar addition on crop soil water infiltration in arid and semiarid regions [19]–[21]. Loosely compacted soil was used in their study considering the requirement of soil respiration for plant growth. Since having distinctive behaviour between agricultural soil and earthwork structure, the further study of biochar application in engineered structured is extremely required.

The aim of this research is to investigate the water infiltration and hydrological behaviour of biochar-amended soil (BAS) under extreme climate scenario. To do this research, three variations of biochar composition (i.e., 0%, 10% and 20%) were observed in this study. Regarding [22], by adding 10% or 20% of biochar implies possible interaction between soil components and biochar and/or the effect of biochar oxidation. Transient numerical simulation analysis using one dimensional axisymmetric idealization was conducted using Seep/W [23]. Further to this, extreme rainfall and drought based on the worst climate scenario (RCP 8.5) occurring in the next 40 years were applied in the simulation. The current climate condition was also analyzed for comparison purposes. Water infiltration rate and cumulative infiltration depth was then observed with respect to biochar variation and climate scenarios. In addition, PWP along the depth was also investigated throughout the simulation. The result of this study will be expected to provide a better understanding of the usage of BAS in earthwork structure, especially under extreme climate scenarios.

2. Methodology

2.1 Model Geometry

In this analysis, numerical study was conducted based on experimental model. One dimensional axisymmetric mode was generated with respect to column with an inner diameter of 280 mm, an outer diameter of 300 mm and a height of 800 mm. Therefore, the half-section of the column was modelled in the simulation (i.e., 0.14-m radius and 0.7-m height) as can be shown in Figure 1. Based on [24], the affected area of rainfall infiltration is less than depth of 0.75m. Three variation of BAS composition namely B0, B10 and B20 have been simulated in this research considering two climate scenarios (i.e., current and future).

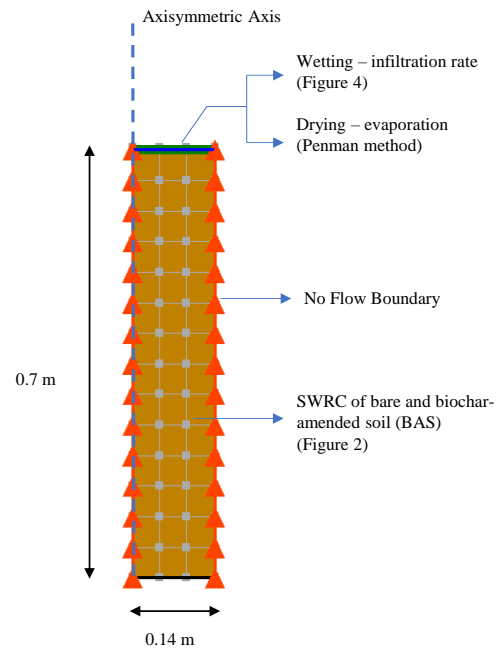


Fig. 1 Model Geometry

2.2 Material Properties

The soil used in the simulation was completely decomposed granite (CDG) which was commonly used as a building material in numerous nations, including Thailand, China, etc. According to the Unified Soil Classification System, the soil was classified as SM because it consists of sand (57.4%), silt (27.6%), and clay (15%). Moreover, the biochar used in this study was ground to pass through a 0.25 mm sieve to provide biochar with a particle size finer than 0.25 mm. Since transient seepage analysis was performed in this simulation, the Soil Water Retention Curve (SWRC) and hydraulic conductivity function (HCF) are crucial and must be incorporated into this model. In the numerical models, drying and wetting SWRC data from the experiment were fitted with the van Genuchten model [25]. Then, HCF were predicted based on SWRC and saturated hydraulic conductivity using equation (1). SWRC data during wetting and drying process can plotted in Figure 2.

$$K_w = K_{sat} \frac{[1 - (a\psi^{(n-1)}(1 + (a\psi^n)^{-m}))^2]}{((1 + a\psi^n)^n)^{\frac{m}{2}}} \quad (1)$$

Where K_{sat} is saturated hydraulic conductivity (m/sec), K_w is unsaturated hydraulic conductivity (m/sec), a , n , m is curve fitting parameters and ψ is matric suction (kPa).

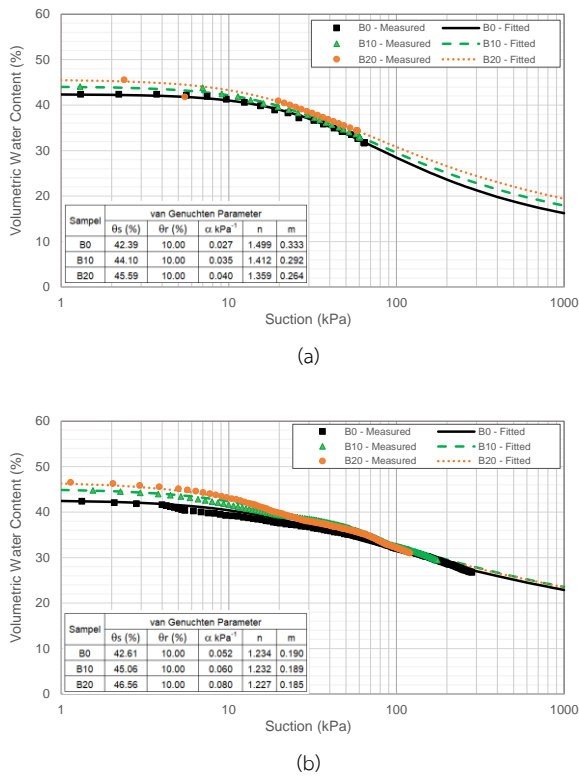


Fig. 2 SWRC (a) Wetting (b) Drying

The SWRC of BAS for bare and biochar-amended soils during (a) wetting and (b) drying conditions is depicted in Figure 2. The addition of biochar can increase the soil's porosity, leading to an increase in its saturated water content. With application rates of 10% and 20%, the saturated water content increased by approximately 2.5% and 4%, respectively. This increase in water content was proportional to the rise in porosity. This increase in water content was proportional to the rise in porosity. Recent research indicates that biochar's abundant pores and large surface area can absorb water during water infiltration, thereby increasing its water-holding capacity [26]. In our study, we did observe slight variations in air-entry values and absorption curves. Despite the increase in pore volume, the size and distribution of pores in BAS were comparable to that of bare soil. This results in a negligible improvement in air-entry values and absorption capacity.

2.3 Boundary Condition

The side boundary was set to no flow, representing an impermeable wall of the column. The bottom boundary was simulated as a review boundary (i.e., boundary reviews for potential seepage faces) during rainfall and no flow (i.e., closed

boundary) during evaporation. To calculate the water flux boundary in relation to precipitation, the Green-Ampt infiltration method was used [27]. The infiltration rate and cumulative infiltration depth can be calculated using equation (2) and (3). In addition, the Penman method [28] was used to calculate evaporation based on the experimental climate data as can be depicted in equation (4). Green-Ampt parameter to calculate water infiltration can be seen in Table 1. Moreover, Penman parameter to calculate evaporation can be shown in Table 2.

$$F(t) = K_{sat} t \cos \beta + \frac{\psi \Delta \theta}{\cos \beta} \ln \left(1 + \frac{F(t) \cos \beta}{\psi \Delta \theta} \right) \quad (2)$$

$$f(t) = K_{sat} \left(\frac{\psi \Delta \theta}{F(t)} + \cos \beta \right) \quad (3)$$

Where, β is slope gradient ($^\circ$), $f(t)$ is infiltration rate (mm/sec), t is time (sec), ψ is suction head (mm), and $\Delta \theta$ deficit of volumetric water content.

$$PET = \frac{0.408 \Delta (Rn - G) + \gamma \frac{900}{T + 273} u_2 (e_s - e_a)}{\Delta + \gamma (1 + 0.34 u_2)} \quad (4)$$

Where PET is Potential Evaporation (mm/day), Rn is Net Radiation (MJ/m²day), G is Soil heat flux density (MJ/m²day), T is Mean daily air temperature at 2 m height ($^\circ$ C), u_2 is Wind speed at 2 m height (m/sec), e_s is saturation vapor pressure (kPa), e_a is actual vapor pressure (kPa), Δ is slope vapor pressure curve (kPa/ $^\circ$ C), γ is psychrometric constant (0.061 kPa/ $^\circ$ C).

Table 1 Green-Ampt parameter

Sample	Current Weather				
	θ_e (%)	K_s (mm/h)	S_e	Δq (%)	i (mm/h)
B0	0.43	4.464	0.430	1.162	29.400
B10	0.44	2.581	0.450	1.169	29.400
B20	0.47	2.041	0.460	1.167	29.400
Sample	Extreme Weather				
	θ_e (%)	K_s (mm/h)	S_e	Δq (%)	i (mm/h)
B0	0.43	4.464	0.430	1.162	30.500
B10	0.44	2.581	0.450	1.169	30.500
B20	0.47	2.041	0.460	1.167	30.500

Table 2 Penman parameter

Sample	Current Weather				
	T (°C)	Rh (%)	Rs (MJ/m ² day)	g (kPa/°C)	Δ
B0	34.00	55	0.092	0.061	0.230
B10	34.00	55	0.092	0.061	0.230
B20	34.00	55	0.092	0.061	0.230
Sample	Extreme Weather				
	T (°C)	Rh (%)	Rs (MJ/m ² day)	g (kPa/°C)	Δ
B0	36.50	54	0.096	0.061	0.260
B10	36.50	54	0.096	0.061	0.260
B20	36.50	54	0.096	0.061	0.260

2.4 Analysis Procedure

A series of numerical analysis using Seep/W was performed to compare the PWP response during rainfall and evaporation events from the experiment. Seep/W is a powerful finite element software product for modeling groundwater flow in porous media. SEEP/W can model simple saturated steady-state problems or sophisticated saturated/unsaturated transient analyses with atmospheric coupling at the ground surface. Each simulation consists of three stages: (i) steady state analysis to set the initial PWP in each model; (ii) transient seepage analysis wherein the models were experienced by rainfall; and (iii) transient seepage analysis due to evaporation under drying process. Initial PWP was set in steady state stages considering the value of PWP at the beginning of the test. To simulate wetting condition, the model was subjected by rainfall with an intensity of 29.4 mm/h for 12 hours. This rainfall intensity was used to simulate the extreme rainfall event corresponding to the 100-year return period in the southern China based on 30 years historical data [29]. Following this, evaporation based on temperature and relative humidity data in the experimental room was applied in the drying simulation for 144 hours. Further to this, extreme rainfall and evaporation induced by extreme climate was also applied to the model. Considering [30] and [31], the air temperature will be increased by 2.5° C in 2060. This can increase cumulative infiltration and also raise surface evaporation.

3. Result and Discussion

3.1 Effects of biochar on infiltration rate

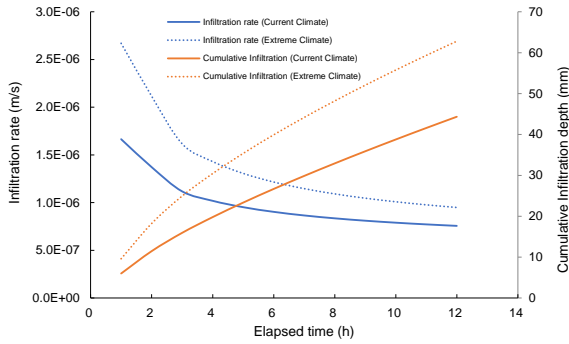
Considering Green-Ampt method, the value of infiltration rate and cumulative infiltration depth along the time can be

calculated and plotted in Figure 3. Figure 3 (a), (b) and (c) correspond to numerical simulation result of biochar content 0%, 10% and 20%, respectively. Moreover, two climate scenarios (i.e., current and extreme climate) can also be seen in the graph. Infiltration rate represent the velocity at which water enter the soil. Meanwhile, cumulative infiltration depth equals the water amount that infiltrated to the soil at specific time. It can be seen from figure 3 that at the beginning of rainfall, the value of water infiltration rate was relatively high correspond to the large difference of hydraulic gradient between upper and lower soil layers. Following this, water infiltration rate was significantly decreased with respect to the decreasing of hydraulic gradient, prior to stable condition. At the commencement of rainfall, the water infiltration rate of BAS column was smaller than bare soil. It can be attributed to the higher value of porosity of BAS column, compared to bare soil. Likewise, water infiltration in BAS was higher than bare soil at the end of rainfall.

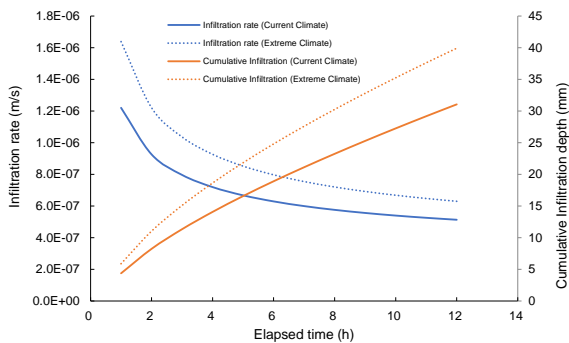
Considering current climate scenario, water infiltration rate for the bare column B0 (i.e., 7.5×10^{-7} m/s) is higher by 39.5% and 53.5% as compared with the B10 (5.2×10^{-7} m/s) and B20 (4.0×10^{-7} m/s), respectively. Further to this, compared to the BAS column, infiltration rate in the bare soil column reached stable faster considering Figure 3. Infiltration rate in B0 was almost stable after 8 h of the simulation, whereas infiltration rate in B10 and B20 was still decreasing. Based on [20], biochar can reduce water infiltration in sandy soil. It can be correlated to pore blockage phenomenon with respect to finer particles of biochar that clog large soil pore, reducing water infiltration rate. Moreover, the value of infiltration rate decreased as the increasing of biochar application. Several studies have also reported that biochar can enhance the soil aggregation [32]. In addition, biochar can be considered as biding agent, leading to flocculate soil particles to form stable aggregates and thus limiting the downward movement of soil water.

Besides, Figure 3 also shows infiltration rate under extreme climate scenario. It can be seen in Figure 3 that infiltration rate under extreme climate tend to have similar pattern with current climate. However, extreme climate resulted higher infiltration rate significantly compared to current climate for all of three BAS variations. Infiltration rate for extreme climate (9.5×10^{-7} m/s) is higher by 25% as compared with current climate at the end of rainfall in bare soil. Moreover, as the increasing of biochar application, extreme climate produced higher infiltration rate by

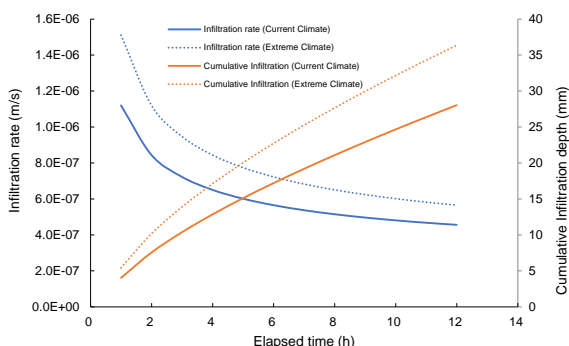
about 22.5% and 23.4% for B10 and B20 respectively compared to current climate. Moreover, in term of extreme climate, water infiltration rate for the bare column B0 is higher by 50.8% and 67.9% as compared with the B10 (6.29×10^{-7} m/s) and B20 (5.65×10^{-7} m/s), respectively.



(a)



(b)



(c)

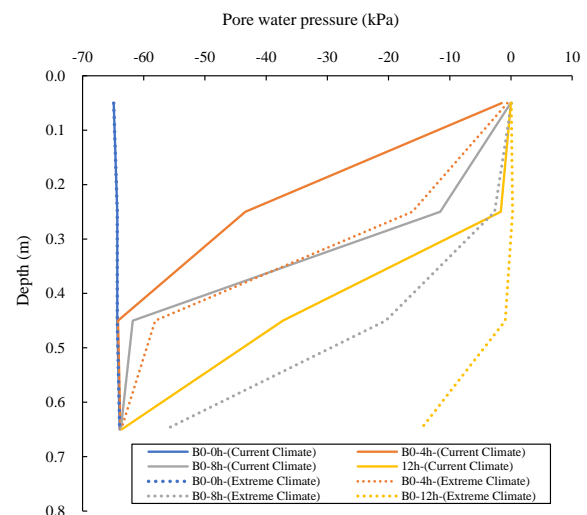
Fig. 3 Infiltration rate and cumulative infiltration (a) B0 (b) B10 (c) B20

3.2 Responses of pore water pressure (PWP) during rainfall at BAS with different biochar application rates.

Regarding the simulation, the response of PWP of three biochar variation at different depth under current and extreme

climate scenario are depicted in Figure 4. In detail, Figure 4 (a), (b) and (c) represent the simulation result of B0, B10 and B20 respectively. PWP data obtained under 4, 8 and 12 h of rainfall represent 2, 10 and 100 years return period respectively regarding [29]. At the beginning of the simulation, initial PWP was set by about -60 kPa following experimental data. As water infiltrate into the soil, the PWP along the depth gradually decreased. As can be seen in Figure 4, the PWP at 0.05 m was close to saturation in all variation of biochar content during 4 h of rainfall, under current climate scenario. The distinctive behaviour occurred at depth of 0.25 m considering the three variations of biochar. PWP at depth of 0.25 was around -43 kPa in bare soil column.

Considering Figure 4, extreme climate scenario triggering remarkable PWP fluctuation, compared to current climate. Due to the higher value of cumulative infiltration depth, PWP at depth of 0.65 dropped by about -14.7 kPa in B0 column, indicating wetting front can reach that depth. Moreover, soil layers above 0.25 became saturation for all biochar variation after 12 h of rainfall. It can also be seen from Figure 4 that PWP increase by about 23 kPa after 12 h of rainfall in B10 column. It indicated that the application of B10 can only prevent water percolation to depth of 0.65. As the application of B20, the soil was more suitable to preventing water percolation up to depth of 0.45.



(a)

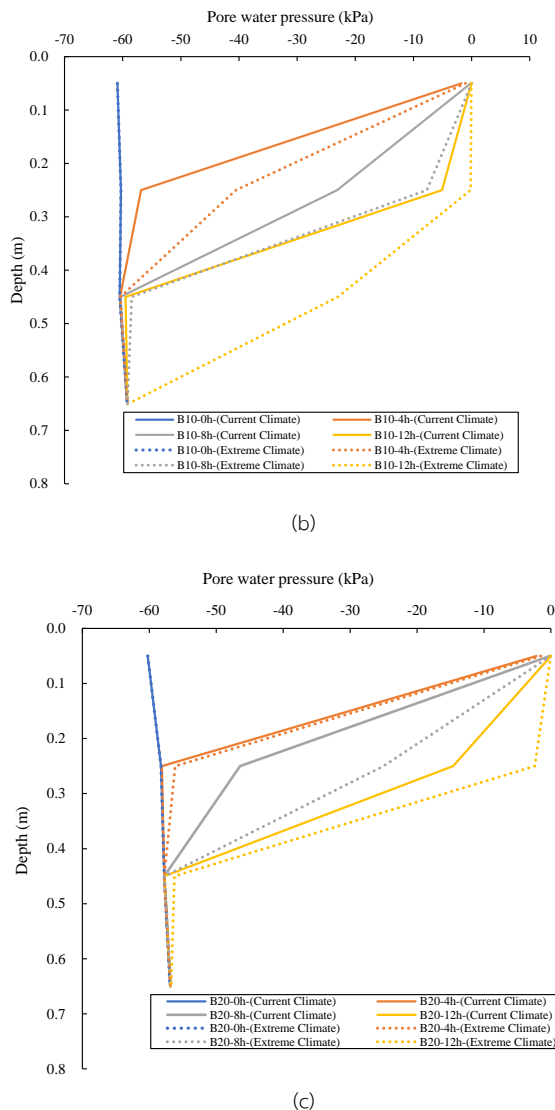


Fig. 3 Development of pore water pressure (PWP) with depth during rainfall (a) B0 (b) B10 (c) B20

3.3 Responses of pore water pressure (PWP) during drying at BAS with different biochar application rates.

The variation of PWP along the depth of three biochar application variation throughout drying process can be depicted in Figure 5. PWP in near surface of bare soil decreased pertaining to evaporation under both current and extreme climate scenario. Considering current climate scenario, soil in the upper half of the column was saturated, based on previous simulation. Following this, PWP decreased after 48 h of evaporation. However, PWP in the lower layer of column was still increase due to the downward infiltration through the column. The downward infiltration process stopped after 48 h of evaporation. Yet, PWP reduced in

entire soil after 48 h of the observation process. At the end of evaporation process, current climate scenario resulted minimum PWP of around -233 kPa at depth of 0.25 m.

According to Figure 5 (b) and (c), it can be reported that the addition biochar tends to have similar trend of PWP behaviour, compared to bare soil. However, the increasing of biochar can reduce the decreasing of PWP during evaporation process. Under current climate scenario, the minimum PWP, located at depth of 0.65 m was only about -175 kPa and -115 kPa for biochar application of 10% and 20%, respectively. It can be attributed to the biochar particles that reduce the large pores and hence minimize soil water evaporation. Moreover, the lower half of column was not significantly influenced of evaporation process in both B10 and B20 column. Based on Figure 5 (b) and (c), the PWP value was remained unchanged at depth of 0.45 m and 0.65 m after 144 h of evaporation process.

Considering extreme climate scenario, the noticeable decreasing of PWP occurred in three biochar variations at near surface depth. The minimum PWP value of bare soil (B0) was about -369 kPa at depth of 0.25 m. It increased by around 58%, compared to current climate scenario. Moreover, the addition of biochar can also reduce the decreasing of PWP significantly under extreme scenario. The minimum PWP at depth of 0.25 m was around 216 kPa and 168 kPa with variation of biochar application of 10% and 20% respectively. It can decrease by around 40% and 54%, compared to B0 variation. In fact, the effect of evaporation to PWP at lower half of column was limited. It can be indicated that biochar can mitigate a very low magnitude of PWP under extreme drought. The biochar can also prevent any significant desiccation cracks [33] and thus avoid deteriorating the performance of soil cover.

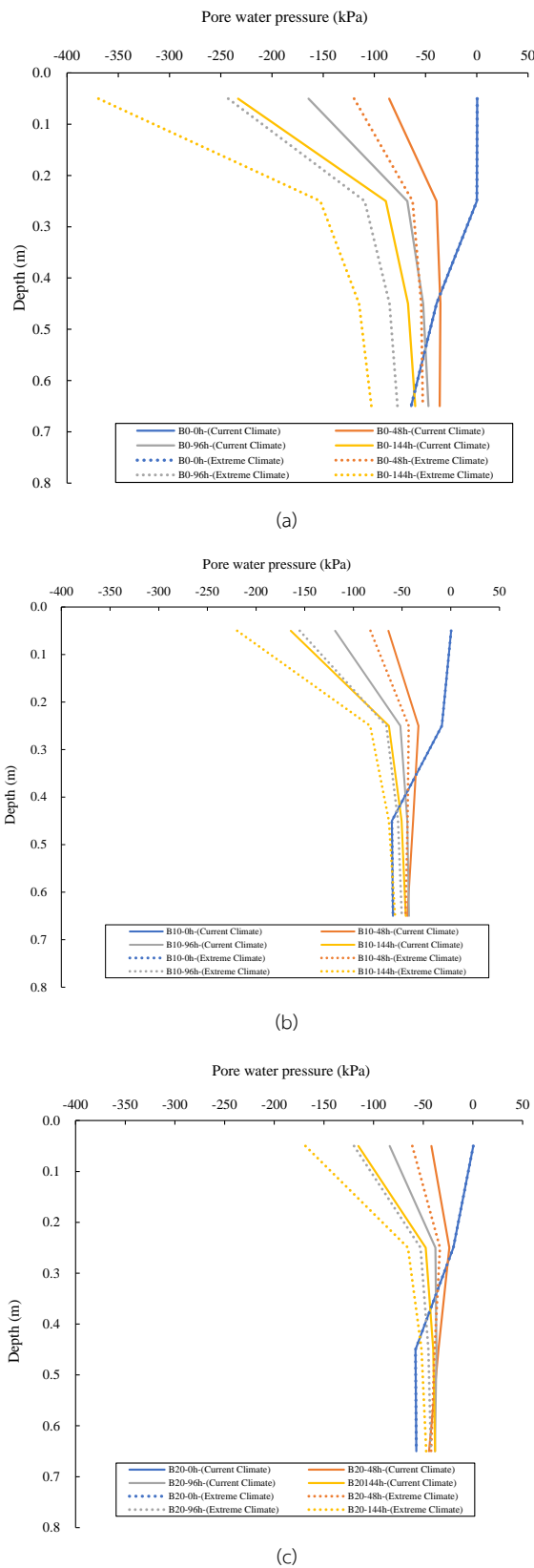


Fig. 3 Development of pore water pressure (PWP) with depth during drying (a) B0 (b) B10 (c) B20

4. Conclusions

In this research, water infiltration and hydrological behaviour due to biochar amended soil (BAS) under extreme climate has been investigated using numerical simulation. Three variation of Biochar composition (i.e., 0%, 10%, dan 20%) has been calculated in this simulation under extreme rainfall, followed by extreme drought. The alteration of water infiltration and pore water pressure were observed and analyzed in this study. The conclusion of the result can be written as follows:

- The increasing of biochar will reduce water infiltration rate significantly. It can be attributed to pore clogging phenomenon with respect to finer particles of biochar that block large soil pore, reducing water infiltration rate.
- Biochar amended soil can significantly reduce the increasing of PWP during infiltration under extreme climate. This is contributed by several factors: (i) the pores of biochar were primarily between 1 – 10 μ m, (ii) the clogging of fine biochar particles and (iii) the soil aggregation induced by biochar.
- The usage of biochar can mitigate very low PWP under extreme drought, preventing extensive cracks and deterioration of soil cover. The biochar application can thus be an eco-friendly and more sustainable approach for soil covers against climate change.

Acknowledgement

The first authors would like to thank the grants No KDS 2020/017 supported by King Mongkut's Institute of Technology Ladkrabang. The corresponding author (V. Kamchoom) acknowledges the grant (FRB66065/0258-RE-KRIS/FF66/53) from King Mongkut's Institute of Technology Ladkrabang (KMITL) and National Science, Research and Innovation Fund (NSRF), the grant (N10A650844) under Climate Change and Climate Variability Research in Monsoon Asia (CMON3) from the National Research Council of Thailand (NRCT) and the National Natural Science Foundation of China (NSFC).

References

- [1] D. G. Fredlund and H. Rahardjo, "Soil Mechanics for Unsaturated Soils," Soil Mech. Unsaturated Soils, 1993, doi: 10.1002/9780470172759.
- [2] G. Ranjan and A. S. R. Rao, Basic and Applied Soil Mechanics. New Delhi: New Age International Publishers, 2000.

- [3] K. M. Briggs, T. A. Dijkstra, and S. Glendinning, "Evaluating the deterioration of geotechnical infrastructure assets using performance curves," *Int. Conf. Smart Infrastruct. Constr.* 2019, ICSIC 2019 *Driv. Data-Informed Decis.*, vol. 2019, pp. 429–435, 2019, doi: 10.1680/icsic.64669.429.
- [4] K. M. Briggs, J. A. Smethurst, W. Powrie, and A. S. O'Brien, "Wet winter pore pressures in railway embankments," *Proc. Inst. Civ. Eng. Geotech. Eng.*, vol. 166, no. 5, pp. 451–465, 2013, doi: 10.1680/gen.11.00106.
- [5] A. Apriyono, Yuliana, and V. Kamchoom, "Serviceability of cut slope and embankment under seasonal climate variations," *Acta Geophys.*, no. 0123456789, 2022, doi: 10.1007/s11600-022-00953-x.
- [6] A. S. Lees, G. J. MacDonald, A. Sheerman-Chase, and F. Schmidt, "Seasonal slope movements in an old clay fill embankment dam," *Can. Geotech. J.*, vol. 50, no. 5, pp. 503–520, 2013, doi: 10.1139/cgj-2012-0356.
- [7] X. Wang, Z. Liu, and H. Chen, "Investigating Flood Impact on Crop Production under a Comprehensive and Spatially Explicit Risk Evaluation Framework," *Agric.*, vol. 12, no. 4, 2022, doi: 10.3390/agriculture12040484.
- [8] G. Kaur, B. Zurweller, P. P. Motavalli, and K. A. Nelson, "Screening corn hybrids for soil waterlogging tolerance at an early growth stage," *Agric.*, vol. 9, no. 2, pp. 1–18, 2019, doi: 10.3390/agriculture9020033.
- [9] A. Collaku and S. A. Harrison, "Losses in wheat due to waterlogging," *Crop Sci.*, vol. 42, no. 2, pp. 444–450, 2002, doi: 10.2135/cropsci2002.4440.
- [10] J. Shaikh, S. Bordoloi, S. K. Yamsani, S. Sekharan, R. R. Rakesh, and A. K. Sarmah, "Long-term hydraulic performance of landfill cover system in extreme humid region: Field monitoring and numerical approach," *Sci. Total Environ.*, vol. 688, pp. 409–423, 2019, doi: 10.1016/j.scitotenv.2019.06.213.
- [11] W. H. Albright, C. H. Benson, G. W. Gee, T. Abichou, S. W. Tyler, and S. A. Rock, "Field Performance of Three Compacted Clay Landfill Covers," *Vadose Zo. J.*, vol. 5, no. 4, pp. 1157–1171, 2006, doi: 10.2136/vzj2005.0134.
- [12] Q. Cheng, C. S. Tang, D. Xu, H. Zeng, and B. Shi, "Water infiltration in a cracked soil considering effect of drying-wetting cycles," *J. Hydrol.*, vol. 593, no. October, p. 125640, 2021, doi: 10.1016/j.jhydrol.2020.125640.
- [13] H. Zeng, C. S. Tang, Q. Cheng, C. Zhu, L. Y. Yin, and B. Shi, "Drought-Induced Soil Desiccation Cracking Behavior With Consideration of Basal Friction and Layer Thickness," *Water Resour. Res.*, vol. 56, no. 7, pp. 1–15, 2020, doi: 10.1029/2019WR026948.
- [14] W. K. Song and Y. J. Cui, "Modelling of water evaporation from cracked clayey soil," *Eng. Geol.*, vol. 266, 2020, doi: 10.1016/j.enggeo.2019.105465.
- [15] Y.-J. Cui, C.-S. Tang, A. M. Tang, and A. N. Ta, "Investigation of Soil Desiccation Cracking using Environmental Chamber," *Riv. Ital. di Geotec.*, vol. 24, no. 1, pp. 9–20, 2014.
- [16] J. A. Kuhn and D. J. G. Zornberg, "Field Suction and Effect of Cracking in Highly Plastic Clay," vol. 7, no. 22, 2006.
- [17] J. T. F. Wong, Z. Chen, X. Chen, C. W. W. Ng, and M. H. Wong, "Soil-water retention behavior of compacted biochar-amended clay: a novel landfill final cover material," *J. Soils Sediments*, vol. 17, no. 3, pp. 590–598, 2017, doi: 10.1007/s11368-016-1401-x.
- [18] A. Garg et al., "Influence of soil density on gas permeability and water retention in soils amended with in-house produced biochar," *J. Rock Mech. Geotech. Eng.*, vol. 13, no. 3, pp. 593–602, 2021, doi: 10.1016/j.jrmge.2020.10.007.
- [19] J. Novak et al., "Biochars impact on water infiltration and water quality through a compacted subsoil layer," *Chemosphere*, vol. 142, pp. 160–167, 2016, doi: 10.1016/j.chemosphere.2015.06.038.
- [20] A. Ibrahim, A. R. A. Usman, M. I. Al-Wabel, M. Nadeem, Y. S. Ok, and A. Al-Omran, "Effects of conocarpus biochar on hydraulic properties of calcareous sandy soil: influence of particle size and application depth," *Arch. Agron. Soil Sci.*, vol. 63, no. 2, pp. 185–197, 2017, doi: 10.1080/03650340.2016.1193785.
- [21] V. Abrol et al., "Biochar effects on soil water infiltration and erosion under seal formation conditions: rainfall simulation experiment," *J. Soils Sediments*, vol. 16, no. 12, pp. 2709–2719, 2016, doi: 10.1007/s11368-016-1448-8.
- [22] J. Jin, M. Kang, K. Sun, Z. Pan, F. Wu, and B. Xing, "Properties of biochar-amended soils and their sorption of imidacloprid, isoproturon, and atrazine," *Sci. Total Environ.*, vol. 550, pp. 504–513, 2016, doi: 10.1016/j.scitotenv.2016.01.117.
- [23] GEO-SLOPE International Ltd, *Seepage Modeling with SEEP/W*, 6th ed., no. July. Alberta, Canada, 2012.

- [24] B. Yuan, Z. Cai, M. Lu, J. Lv, Z. Su, and Z. Zhao, "Seepage analysis on the surface layer of multistage filled slope with rainfall infiltration," *Adv. Civ. Eng.*, vol. 2020, 2020, doi: 10.1155/2020/8879295.
- [25] M. T. Van Genuchten, "A Closed-form Equation for Predicting the Hydraulic Conductivity of Unsaturated Soils," *Soil Sci. Soc. Am. J.*, vol. 44, no. 5, pp. 892–898, 1980, doi: 10.2136/sssaj1980.03615995004400050002x.
- [26] K. C. Uzoma, M. Inoue, H. Andry, H. Fujimaki, A. Zahoor, and E. Nishihara, "Effect of cow manure biochar on maize productivity under sandy soil condition," *Soil Use Manag.*, vol. 27, no. 2, pp. 205–212, 2011, doi: 10.1111/j.1475-2743.2011.00340.x.
- [27] W. H. Green and G. A. Ampt, "Studies on Soil Physics," *J. Agric. Sci.*, vol. 4, no. 1, p. 1, 1911.
- [28] H. L. Penman, "Natural evaporation from open water, bare soil and grass," *Proc. R. Soc. Lond. A. Math. Phys. Sci.*, vol. 193, no. 1032, pp. 120–145, 1948, doi: 10.1098/rspa.1948.0037.
- [29] G. of H. K. Drainage Service Department, "Stormwater Drainage Manual 2015," no. January, 2018, [Online]. Available: <https://docs.lib.purdue.edu/intappubs/100/>.
- [30] G. Krinner et al., "Long-term climate change: Projections, commitments and irreversibility," *Clim. Chang. 2013 Phys. Sci. Basis Work. Gr. I Contrib. to Fifth Assess. Rep. Intergov. Panel Clim. Chang.*, vol. 9781107057, pp. 1029–1136, 2013, doi: 10.1017/CBO9781107415324.024.
- [31] World Bank Group, "Climate Risk Country Profile: China," 2021. [Online]. Available: www.worldbank.org.
- [32] C. George, M. Wagner, M. Kücke, and M. C. Rillig, "Divergent consequences of hydrochar in the plant-soil system: Arbuscular mycorrhiza, nodulation, plant growth and soil aggregation effects," *Appl. Soil Ecol.*, vol. 59, pp. 68–72, 2012, doi: 10.1016/j.apsoil.2012.02.021.
- [33] Z. Chen, V. Kamchoom, and R. Chen, "Landfill gas emission through compacted clay considering effects of crack pathway and intensity," *Waste Manag.*, vol. 143, no. April, pp. 215–222, 2022, doi: 10.1016/j.wasman.2022.02.032.